Epidemics in the presence of social attraction and repulsion

Evelyn Sander

Department of Mathematical Sciences

George Mason University, Fairfax, VA 22030, USA

Chad M. Topaz

Department of Mathematics, Statistics, and Computer Science

Macalester College, St. Paul, MN 55105, USA

(Dated: October 1, 2010)

Abstract

We develop a spatiotemporal epidemic model incorporating attractive-repulsive social interactions similar to those of swarming biological organisms. The swarming elements of the model describe the ability of distinct classes of individuals to sense each other over finite distances and react accordingly. Our model builds on the non-spatial SZR model of [Munz, Hudea, Smith?, 2009] modeling a specific epidemic, namely the attack of zombies. This case is interesting from the modeling standpoint, as zombie epidemics are particularly virile, albeit restricted to a theater near you and certain parts of San Francisco, Washington D.C., and other major metropolitan areas [http://www.zombiewalk.com]. Spatial effects not only enhance entertainment value (as a cinematic portrayal of a spatially invariant zombie attack would be somewhat lacking in thrill) but are critical to understanding the epidemic. We show that in the absence of a cure for zombiism, the alert human population will eventually be annihilated, but at a slower rate than in the non-spatial model. The extra time to extinction might allow the development of a cure. We also show that without any assumption of collusion, the system self-organizes into transient traveling pulse solutions consisting of a swarm of zombies in pursuit of a swarm of alert humans. In the presence of a zombie cure, the traveling solutions exist persistently and stably for all time.

PACS numbers: 87.10.Ed,87.19.X-,87.23.-n

I. INTRODUCTION

The notion of a zombie has its roots in the African Kingdom of Kongo, from whence the African diaspora brought it to Haiti. In Haitian voodoo, a sorcerer (or *boko*) could force someone (either living or dead) to become a zombie, while the boko maintained control of the soul. In contrast, the more modern view of zombiism is that it does not result from a sorcerer's control, but rather is an uncontrolled and unmodulated epidemiological effect, spread via contact like a disease. This "viral" zombiism is depicted the classic 1968 movie *The Night of the Living Dead*, in Michael Jackson's 1993 music video *Thriller*, in the computer game *Plants versus Zombies*, and at public events such as zombie walks and the game *Humans vs. Zombies* played on many college campuses.

On the scientific front, in 2009, [1] first quantified the epidemiological view of zombies. This work (of which we later provide a detailed discussion) adapted classical epidemiological models to predict the course and ultimate outcome of zombie attacks. This important, foundational zombie modeling effort focused on the zombification of a population of healthy alert humans, but did not consider any geographic or spatial information pertaining to zombie attacks. Of course, spatial information is often critical for understanding how to effectively treat an epidemic. For example, consider the citizens of Copenhagen in 1349, during the bubonic plague. A year later, the epidemic arrived in the city and spread explosively. Knowledge that the epidemic front was moving steadily northwards in an east-west band from the south [2] would have been much more actionable for Copenhangen's citizens than only knowing that the epidemic was adversely effecting the total population of Europe.

In this paper, we develop an epidemiological model of zombies which addresses the need for spatial information. Ours is not the first epidemiological model to treat spatial effects. However, most such models have incorporated spatial effects using the concept of spatial diffusion, via which individuals are modeled to move at random, with each interaction with an infected individual resulting in a potential spread of the infection. In contast, random motion is not an appropriate assumption for the case of zombies, who by nature seek out healthy humans as prey. Thus, our modeling methods will necessarily be different.

One aspect of the standard epidemiological models that we do adopt here is the *mean field hypothesis*, which says that the behavior of individuals can be understood by considering a continuous function describing average behavior. From day-to-day observations of fluids, one

finds it perfectly plausible that their flow and motion can be modeled (for most applications) by such averages, rather than by keeping track of the motion of individual molecules. One might wonder if this is a reasonable modeling assumption to make about the macroscopic behavior of populations of complex biological organisms. In fact, such an assumption does prove to be quite successful in many situations, and the mean field approach in biology is supported by a substantial literature tracing its roots (at least) back to work such as [3, 4]. As a visual example, consider the crowd phenomenon "the human wave" in a stadium. Although each individual initiates an individual action to stand and sit, the macroscopic effect resembles the motion of a fluid wave.

We now return to the question of how to model zombies, keeping in mind that their motion is mostly directed, rather than purely random. Our goal is to address the observation that zombies can behave in an organized fashion, for instance, pursuing humans in packs. One possible explanation is that their behavior is being controlled, with the control exerted by someone such as the a traditional Haitian boko. However, as mentioned before, such control is not part of the modern viewpoint of zombies. In a modern zombie epidemic there would be no external controlling force. A second possible explanation is collusion, that is, the agreement of a master plan amongst the zombies (or perhaps as assigned by a zombie leader). We discard this possibility as well, due to the minimal brain power possessed by zombies. They may have the brain power of a fish or a bird, but certainly not sufficient mental capacity to design any sophisticated strategy of directed attack. Consider however that both birds and fish can behave in organized schools and swarms, and that these behaviors arise without control or collusion. A body of mathematical research has successfully modeled such swarming and flocking behavior. The key model element is that each individual is able to sense the behavior of others within reasonably close proximity, and to instinctively react accordingly. The result of the reaction to local behavior is that the population spontaneously organizes itself into a structure such as a swirling school of fish, a directed flock of birds, or a traveling wave of sitting-and-standing humans in a sports arena.

Based on the successes of the swarm modeling approach, the spatial aspects of the epidemiological model we will present are adapted from the swarming literature, with the assumption that each individual zombie is attracted to populations of alert humans, and each alert human is repelled by zombies. Our primary result is that the population self-organizes into swarms of zombies pursuing humans. If there is no cure for zombiism, the

alert human population eventually dies out, but not as quickly as predicted by a non-spatial epidemic model. However, in the presence of a cure, it is possible for a population of zombies to stably pursue a population of alert humans for all time – a traveling wave. In addition, we find many other types configurations of zombies in pursuit, with humans on the run. Much can be gained by full knowledge of these different moving population configurations, and the likelihood of successful persistence of the alert human population. Specifically, an understanding of the types of behavior possible and how to recognize their onset is critical for purposes planning and preparation for large scale epidemiological events.

The remainder of this introduction consists of a detailed and more technical overview of the body of scientific literature on epidemiological models and swarming models, and a description of how our modeling fits into this framework.

Epidemiological modeling in perspective. Though the history of epidemic modeling reaches back to studies of smallpox in the mid-18th century [5, 6], the incorporation of spatial effects has roots in the last hundred years. Spatial epidemic models are reviewed, *e.g.*, in [7–9]. One major class of spatial models treats the population as a continuum in space and tracks the population density in space and time (per the mean field assumption discussed above). Within this realm of continuum models, the most basic studies of spatial epidemics modify non-spatial differential equation based compartmental models, which divide a population into different epidemiological classes such as susceptible, infected, and recovered. The basic spatial models add simple diffusion as the macroscopic description of the underlying random motion of individuals within a population [10–12], and focus on the propagation of epidemic fronts from a clustered initial condition of infected individuals. A generalization of these models is the distributed infectives model [13, 14] which incorporates dispersal that is longer-range than that described by diffusion. Another class of models uses spatial terms to describe not the movement of the individuals, who are now assumed to be stationary, but rather the transmission of the disease itself. For instance, in the distributed contacts model [15–17] the infectivity at each point in space is computed from a weighted spatial average of the field of infected individuals over long ranges.

Most short-range spatial effects can be modeled with mathematical terms that involve spatial derivatives, which compute rates of change of a quantity over an infinitesimal spatial range. One intuitive example is that of chemotaxis [18]. In a simple chemotactic situation, a biological organism such as a bacterium senses a chemical field (perhaps a nutrient field)

immediately surrounding it and moves in the direction of greatest increase. In contrast, long-range effects such as those in the distributed infectives and distributed contacts models cannot be accurately described with spatial derivatives. Instead, one typically uses so-called nonlocal operators such as integral operators, which compute quantities over finite (or potentially infinite) ranges.

Swarming models. We introduce a spatial model for epidemics in which nonlocal terms capture a completely different effect from those previously examined. In particular, we will model the directed motion of individuals due to social forces in an epidemiological context. By social forces, we mean forces such as attraction to and repulsion from other members of the population. These forces have received substantial attention in studies of swarming groups such as fish schools, bird flocks, and insect plagues; see the literature reviews in [19–21] and others. In the traditional biological swarming context, attraction and repulsion operate simultaneously between conspecific organisms. Some fish, for example, are evolutionarily preprogrammed with attraction, which provides safety and group cohesion, and repulsion, which helps avoid collisions. The balance between the two forces typically leads to a preferred separation distance between neighboring organisms in a group. Social forces may arise directly from organisms' sensing over finite distances via sound, sight, smell, or touch, or indirectly via chemical or other signals.

We now turn our attention to zombie epidemics in the presence of social forces. The recent work of [1] was the first to develop a mathematical model for zombie epidemics. It concluded that in the absence of a cure, the only possible outcome of a zombie epidemic is complete annihilation of the healthy, alert human population. However, as we have mentioned, by neglecting spatial features, the original model leaves open a key question of zombie epidemics, namely that of how a swarm of zombies self-organizes to pursue and attack a swarm of self-organized healthy humans without any collusion on the part of either the zombie or the alert human populations. We will probe this phenomenon by generalizing the model of [1] to include spatial variation, and in particular by incorporating social interaction terms. These terms account for zombies being socially attracted to healthy humans, and healthy humans being socially repulsed from zombies.

Organization of the paper. The rest of this paper is organized as follows. In Section II we construct our model. In Section III, we examine some of its basic properties. The model conserves total population, but does not conserve center of mass. We then consider

mass balanced states and show that spatial coexistence of healthy humans and zombies is impossible. Finally, we show that the only possible steady states are homogeneous in space, and we compute their stability. In Section IV we perform numerical simulations of our model, focusing on the effect that the spatial terms have vis-a-vis the non-spatial model. Though the spatial and non-spatial models reach the same doomsday equilibrium in which zombies extinguish healthy humans, the approach to the equilibrium can be slower in the spatial case. Furthermore, in the spatial case, the population can self-organize into a traveling pulse of susceptible humans that is pursued by a group of zombies. Though the pulse is merely transient, it is possible that the added time necessary to reach the doomsday equilibrium would afford the opportunity to develop a cure for zombiism. In Section V we consider an extension of the model in which such a cure exists, again examining equilibria and their stability. In Section VI, we perform numerical simulations for this case of a cure and show that traveling solutions can persist stably. Finally, we conclude in Section VII with some open questions for the zombie research community.

The model we will develop and the mathematical tools we will use to study it draw from partial differential equations, dynamical systems, and analysis. However, we strive to keep mathematical details to a minimum in the body of our paper. For the material presented in Sections II through VI, we focus our presentation on the main ideas; the reader who is especially mathematically-inclined will find details and derivations in the appendices.

II. MODEL CONSTRUCTION

We begin by reviewing the following spatially homogeneous SZR model of [1]:

$$\dot{S} = \Pi S - \beta SZ - \delta S, \tag{1a}$$

$$\dot{Z} = \beta SZ + \zeta R - \alpha SZ, \tag{1b}$$

$$\dot{R} = \delta S + \alpha SZ - \zeta R. \tag{1c}$$

The total population consists of three classes of individuals: active alert humans, denoted by S, zombies, who are deceased reanimated humans, denoted by Z, and those who are recently deceased but not reanimated, and thus are removed from either alert human or zombie populations, denoted by R. Each over-dot in (1) represents a time derivative. The

right-hand sides represent rules for the instantaneous rates of change of the number in each different population class.

Members of the healthy human population are susceptible to becoming zombies as a direct result of an encounter with a zombie, with a zombie bite as the usual mechanism of transmission. The recruitment of alert humans to the zombie population occurs via mass-action kinetics with transmission parameter β. The mass-action kinetics assumption means, for instance, that the rate at which alert humans are bitten by zombies is proportional to the rate of contact between the two different classes. This is in turn assumed to be proportional to the product of the number of individuals within each class, hence giving rise to the product SZ in (1). Though the model uses the law of mass action, in future studies one could modify this to be the standard incidence model, which assumes that the contact rate is not dependent on the total population size (see, *e.g.*, [7]).

The zombification of the removed population R is independent of social interaction as the members of this class are deceased and inanimate. It is assumed to be directly proportional to R with proportionality constant ζ, the natural undeath rate for reanimation of recently deceased humans. In addition to the two routes into the zombie class, it is possible for zombies to join the removed class as a result of an altercation between a zombie and a healthy, alert human in which the latter triumphs. Once again, this route from Z to R occurs via mass action, with altercation rate α.

The model above incorporates the fact that independent of zombie interaction, the susceptible class has natural birth and death rates, denoted respectively by Π and δ. However, compared to the time scale of a zombie epidemic, these effects are negligible and one can set $\Pi = \delta = 0$ as in [1]. Therefore, the total population size $N = S + Z + R$ is fixed, and the equations become

$$\dot{S} = -\beta SZ, \tag{2a}$$

$$\dot{Z} = \beta SZ + \zeta R - \alpha SZ, \tag{2b}$$

$$\dot{R} = \alpha SZ - \zeta R. \tag{2c}$$

Governing equations. The model (2) neglects the spatial structure of the zombie epidemic. We now construct a spatiotemporal version of this model. As discussed in Section I, the most basic spatial models of epidemics incorporate linear diffusion, modeling the random

movement of individuals; see, *e.g.*, [10–12]. However, such an assumption is insufficient to model zombie epidemics in that it does include any directed motion. Crucial to the understanding of interactions between zombies and alert humans is the fact that zombies tend to be attracted to alert humans, and alert humans seek to avoid zombies. Furthermore, the attraction and repulsion are not local effects. As with many socially interacting populations, both zombies and humans can sense population densities on finite (rather than infinitesimal) distances. Hence, we will need to incorporate into our model swarming-type social interaction terms such as those discussed in Section I and used commonly in the biological swarming literature; see, *e.g.*, [19, 20].

In mathematical models of swarms, one commonly assumes that social interactions take place in a pairwise, linear manner, so that to compute the total social force on a given organism, one adds the interaction force between it and each other organism. Continuum swarming models, then, typically involve convolution-type integral terms of the form

$$\int \mathbf{K}(\mathbf{x}-\mathbf{y})\rho(\mathbf{y},t)\,d\mathbf{y} \equiv \mathbf{K} * \rho, \tag{3}$$

where $\rho(\mathbf{x},t)$ is population density and $\mathbf{K}$ is a kernel in which are embedded the rules for social interaction as it arises from sensing; that is, $\mathbf{K}$ gives the effect that organisms at location $\mathbf{y}$ have on those at location $\mathbf{x}$. Some methods of sensing, such as sound, are essentially omnidirectional. Others, such as sight, are more unidirectional. Because many organisms process a combination of communication signals, one often assumes that communication is omnidirectional [21, 22]. Another common assumption is that distinct organisms exert equal and opposite social forces on each other.

The simplest continuum swarming model assumes the total population is conserved (*e.g.*, no birth or death) and neglects intertia. In this case, the population is governed by the conservation equation

$$\dot{\rho} + \nabla \cdot (\rho \mathbf{v}) = 0, \quad \mathbf{v} = \mathbf{K} * \rho. \tag{4}$$

In a one-dimensional domain, the aforementioned assumptions of omnidirectional communication and equal-and-opposite forces cause the social kernel $\mathbf{K} = K$ to be odd. Negative values of $\mathrm{sgn}(x)K(x)$ correspond to attraction and positive values to repulsion. Recently, [20] explored the manner in which the asymptotic dynamics of (4) in a one-dimensional domain depend on properties of K.

Using these ideas from biological swarming, we now modify the non-spatial zombie epidemic model (1). We only include spatial terms in the equations for S and Z, since the individuals in the removed class are deceased and not animated, and are thus completely immobile. Our model is

$$\dot{S} + \nabla \cdot (v_S S) = D_S \Delta S - \beta SZ, \tag{5a}$$

$$\dot{Z} + \nabla \cdot (v_Z Z) = D_Z \Delta Z + \beta SZ + \zeta R - \alpha SZ, \tag{5b}$$

$$\dot{R} = \alpha SZ - \zeta R, \tag{5c}$$

where S, Z, and R are functions of x and t and are now interpreted as population densities. The parameters D_S and D_Z are the diffusion constants measuring the random motion of susceptibles and zombies. For simplicity, we restrict attention to one-dimensional spatial domains so that $\Delta \equiv \partial_{xx}$ and $\nabla \cdot \equiv \partial_x$.

Since susceptible individuals flee from zombies, we describe susceptibles' velocity due to social interaction as

$$v_S = K_S * Z, \quad K_S = \mathrm{sgn}(x) \cdot F_S e^{-|x|/\ell_S}. \tag{6}$$

Here, K_S is a repulsive kernel, where F_S and ℓ_S describe the characteristic strength and length scale of repulsion. We have chosen K to be a simple kernel capturing the essential property that a susceptible's reaction to a zombie should decay with the distance between the two, due to the limitations of human sensing. Similarly, we model the zombies' advective velocity as

$$v_Z = K_Z * S, \quad K_Z = -\mathrm{sgn}(x) \cdot F_Z e^{-|x|/\ell_Z}, \tag{7}$$

so that zombies are attracted to susceptibles. Figure 1 shows an example of the velocities v_S and v_Z for given population density profiles. We assume that $F_Z \leq F_S$, so that alert humans are more violently repelled by oncoming zombies than zombies are attracted to humans. The opposite assumption would result in a faster velocity of zombies than susceptibles, and in turn the speedy annihilation of the entire susceptible population. We also assume that $\ell_Z \leq \ell_S$, that is, zombies generally sense with less acuity than susceptibles due to their lower level of brain function.

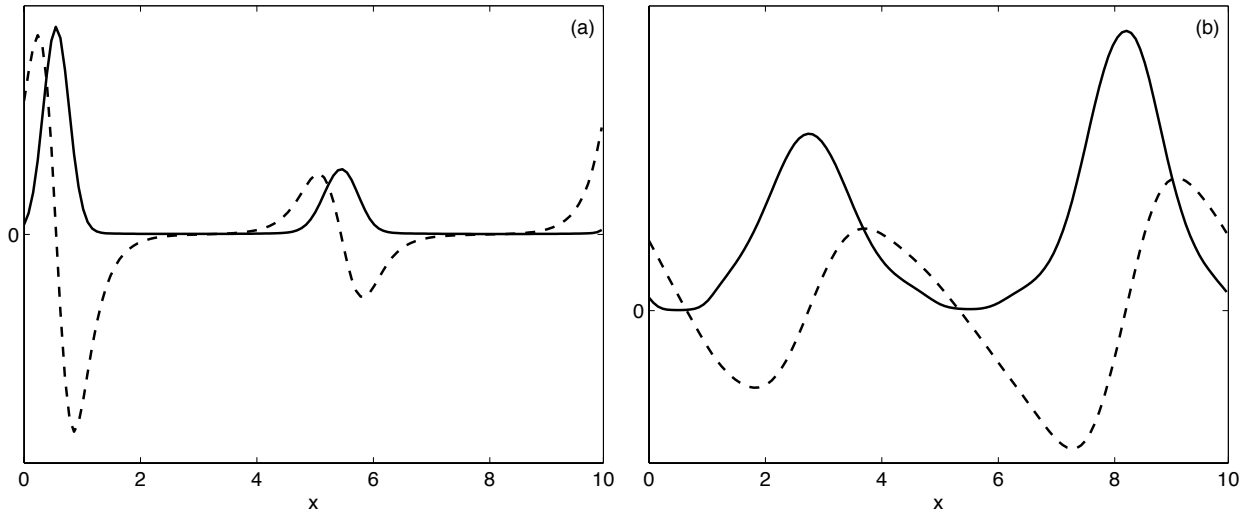

FIG. 1: **Social advection velocities.** Schematic of typical populations plotted with the corresponding nonlocally-determined advective velocities; see Equations (6) and (7). (a) Susceptible population S (solid) plotted with the rescaled zombie velocity $v_Z(S)$ (dashed). Zombies are attracted to susceptibles and move towards maxima of S. (b) Zombie population Z (solid) plotted with the rescaled susceptible velocity $v_S(Z)$ (dashed). Susceptibles are repelled from zombies and move outwards from maxima of Z. Though the population density fields have different units than the velocity fields, we have plotted them on the same axes for a qualitative schematic comparison.

Plugging (6) and (7) into (5), we have our full equation

$$\dot{S} + (SK_S * Z)_x = D_S S_{xx} - \beta SZ, \tag{8a}$$

$$\dot{Z} + (ZK_Z * S)_x = D_Z Z_{xx} + \beta SZ + \zeta R - \alpha SZ, \tag{8b}$$

$$\dot{R} = \alpha SZ - \zeta R. \tag{8c}$$

Nondimensionalization. Nondimensionalization is a standard mathematical technique which involves making a change of variables to remove the physical dimensions (such as length, time, and mass) from an equation in order to obtain a simpler model, possibly by reducing the number of model parameters. This reduction is convenient for analysis and for numerical simulation. One can always re-cast results in dimensional form simply by reversing the change of variables, without any loss of information. The nondimensionalization

procedure for our model appears in Appendix A. The dimensionless model is

$$\dot{S} + (SK_S * Z)_x = D_S S_{xx} - \beta SZ, \tag{9a}$$

$$\dot{Z} + (ZK_Z * S)_x = D_Z Z_{xx} + \beta SZ + R - \alpha SZ, \tag{9b}$$

$$\dot{R} = \alpha SZ - R. \tag{9c}$$

K_S and K_Z have been redefined as

$$K_S = \mathrm{sgn}(x) \cdot e^{-|x|}, \tag{10a}$$

$$K_Z = -\mathrm{sgn}(x) \cdot F e^{-|x|/\ell}. \tag{10b}$$

The dimensionless parameters $F \leq 1$ and $\ell \leq 1$ measure, respectively, the relative strength and length scale of attraction to repulsion. The parameters D_S, D_Z, α, and β are dimensionless versions of the corresponding parameters from the original dimensioned model.

Boundary conditions. Since the governing equations (9) are a spatial model, one must specify a spatial domain and set appropriate boundary conditions, which dictate the behavior of the model at the boundary of the domain. To facilitate our analysis and our computation, we assume that the domain is a finite interval with periodic boundary conditions. To get insight into the behavior for very large domains, one can always choose L very large and focus on the middle of the domain where the finite-size and boundary effects are presumed to be small. For specificity, let the domain be the interval $[0, L]$. Then solutions for S have $S(0) = S(L)$, and $S_x(0) = S_x(L)$, with similar conditions for Z and F. In addition, the length scale of the interaction is assumed extremely small compared to L. Thus, we modify our kernel functions K_S and K_Z to be periodic and this has little effect on their values. That is, outside a small region near their centers, K_S and K_Z are very close to zero.

III. BASIC MODEL PROPERTIES

We now examine some basic properties of (9), seek mass balanced states and spatially homogeneous steady states, and calculate the linear stability of the latter. We also show that spatially homogeneous steady states are the only possible steady states.

Conservation of total population. By construction, the total population size (alert humans, the dead, and the undead all combined) should remain unchanged under the dynamics of (9). If we denote the population size at each point by $n(x,t)$ and the total population size as $N(t)$,

$$n(x,t) = S + Z + R, \tag{11}$$

$$N(t) = \int_0^L n(x,t)\, dx, \tag{12}$$

then conservation of population means that N is constant, as in [1]. Appendix B derives the conservation of population – or as we will sometimes say, conservation of mass – for the model (9). For the remainder of this paper, we treat the population size N as an additional parameter in the model.

Center of mass and traveling solutions. One question of interest throughout the rest of this paper pertains to the ability of the population to migrate under the dynamics of the model. One simple way to touch upon this question is to determine whether the center of mass of the population can move, or whether it must be stationary. In qualitative terms, the center of mass of the population is defined as the average of the positions of all of the individuals within the population. A proof that the center of mass remains stationary would mean that solutions consisting the population translating in one direction would be impossible. We show in Appendix C that, in fact, the center of mass can migrate. This means that traveling solutions are not *a priori* ruled out, although in our numerical simulations of (9) we have only found transient traveling solutions; see Figures 2(a) and 3(a-c). In Appendix C we calculate the center of mass to show that the center of mass can travel with a nonzero speed.

Mass balanced solutions, steady states, and stability. We now turn our attention to different types of equilibria of (9). Though a system such as (9) could, in theory, have long-term behavior more complicated than an equilibrium, equilibria are some of the most fundamental long-term behaviors one might wish to study.

We are first interested in mass balanced states. By mass balanced states, we mean states where the number of individuals within each class is not changing in time. It is important to note that even in such a state, the solution itself could still be changing (for instance, imagine a group of fixed population count traveling in space). However, finding mass balanced states

would still provide useful information for epidemiological tallies. In Appendix D, we show that at mass balance, $R = 0$, meaning there are no deceased individuals. All individuals are alert humans or zombies. Furthermore, we show that either $S = 0$ or $Z = 0$ at every point in space. This means that alert humans and zombies cannot co-exist at the same spatial location.

Now consider steady-states of (9). Steady states are states for which the time derivatives vanish, meaning that the solutions do not change in time. This is a more restricted class of solutions than mass balanced states. That is, while every steady state is a mass balanced state, not every mass balanced state need be a steady state.

In Appendix E we show that the only possible steady states are spatially homogeneous ones, that is, solutions where not only is the mass balanced, and not only are the solutions no longer changing in time, but there is no spatial variation in the profile. The steady state solutions have population density within each class S, Z, R that is constant in space. The two steady state solutions are the susceptible state

$$(S^*, Z^*, R^*) = (N/L, 0, 0), \tag{13}$$

and the doomsday state

$$(S^*, Z^*, R^*) = (0, N/L, 0), \tag{14}$$

in which all individuals have become zombies. To obtain the mass balance for each steady state (that is, the number of individuals within each class) one must integrate over the spatial domain. For (13) the mass balance is

$$\int_0^L S^*\,dx = N, \quad \int_0^L Z^*\,dx = 0, \quad \int_0^L R^*\,dx = 0, \tag{15}$$

and for (14) it is

$$\int_0^L S^*\,dx = 0, \quad \int_0^L Z^*\,dx = N, \quad \int_0^L R^*\,dx = 0. \tag{16}$$

These are the same mass balances as the steady states of the non-spatial model of [1]. We have not established whether (9) has other attractors such as inhomogeneous steady states and traveling waves. Our numerical investigations (described at greater length in Section IV)

show transient traveling solutions, but have not revealed any long-term behavior other than the spatially homogeneous states.

We conclude this section with a study of the linear stability of the two spatially homogeneous steady states (13) and (14). We review the concept of linear stability of solutions to partial differential equations with the following (nonmathematical) thought experiment. Imagine taking an equilibrium solution for (S, Z, R) and applying a very small spatial perturbation to the solution profile. If all such small (in fact, infinitesimal) perturbations decay over time so that the system again reaches the equilibrium, then we say the equilibrium is linearly stable. If any such perturbations grow in time, then the equilibrium is unstable. The stability properties of equilibria are crucial for us because they give hints about the possible long-time consequences of zombie epidemics. A stable equilibrium has the hope of being reached in the long-term if the system begins at some non-equilibrium state (though it is not guaranteed). An unstable equilibrium can never in practice be reached (since tiny perturbations and fluctuations will always be present in real systems).

The calculation of the linear stability of the equilibria (13) and (14) appears in Appendix F. We show that (13) is linearly unstable to generic noisy perturbations (at least, for L sufficiently large). This means that the state in which all individuals are healthy humans cannot be regained if any zombies are introduced into the population. On the other hand, the doomsday state (14) is linearly stable. These stability properties are the same as for the non-spatial model in [1].

IV. NUMERICAL SIMULATIONS AND DISSIPATING TRAVELING PULSES

In this section we present results of numerical simulations of (9). Our numerical scheme is spectral in space, taking advantage of the periodic domain. We treat the nonlocal (convolution) terms via multiplication in Fourier space, and we compute the reaction terms pseudospectrally in real space. Time integration in Fourier space uses MATLAB's built-in timestepper ODE45). For the zombie epidemiologist interested in conducing her or his own simulations, our MATLAB code is available at `http://www.macalester.edu/~ctopaz/zombieswarm.m`.

Figure 2 compares the total number of individuals in each class S, Z, and R as a function of time for three different models. Figure 2(a) corresponds to the full spatial model (9). The

epidemiological parameters are $\alpha = 0.005$ and $\beta = 0.0095$ as in [1], and we take $F = 0.01$, $\ell = 0.02$, $D_S = 0.1$, $D_Z = 0.05$, and $L = 10$. Figure 2(b) is similar, but has the social interaction terms turned off, *i.e.*, $K_S = K_Z = 0$. Both simulations are begun with initial populations

$$\int_0^L S\,dx = 500, \quad \int_0^L Z\,dx = 3, \quad R = 0, \tag{17}$$

with S and Z distributed randomly in space. Despite the difference in the spatial effects for these two situations, the time evolution of the total number in each compartment is strikingly similar. Both models approach the doomsday equilibrium (14) and take equally long to do so. This can be understood by examining linear stability results in Appendix F. From (F12) and (F15), diffusive terms affect the linearization around the susceptible and doomsday equilibria, but the social terms do not. Our simulations begin close to the susceptible equilibrium and conclude at the doomsday one. This suggests that the system spends most of its time in regimes where the linearizations are good descriptions, and hence that social interactions are only transiently important. Despite the similarity of Figures 2(ab), the actual solution profiles for the two cases are markedly different, and we discuss these momentarily. Before doing so, we consider the non-spatial model of Figure 2(c). The decay of the susceptible population is much faster. In fact, by the time the susceptible population has been extinguished in the non-spatial model, susceptibles within the spatial model have barely been impacted by the zombies.

Figure 3 shows S, Z, and R profiles in space-time corresponding to the simulations of Figures 2(ab). For the full model, shown in Figure 3(a-c), the solution shows transient traveling pulses, which are apparent as streakiness in the picture. These pulses are absent in the diffusion-only case, shown in Figure 3(d-f).

We conclude from our numerical explorations that persistence of the healthy human population is impossible within the framework of (9). In all variations of the model considered here, the zombie population eventually overtakes the susceptible population, leading to the doomsday state. However, the manner of approach is important. Spatial effects can slow the decline of the healthy human population, and furthermore, social attraction and repulsion provide for spatial localization of susceptibles and zombies. In the event of a zombie attack, the added time to extinction might allow the healthy, alert humans to seek a cure for zombiism. We consider the effect of such a cure in the next section.

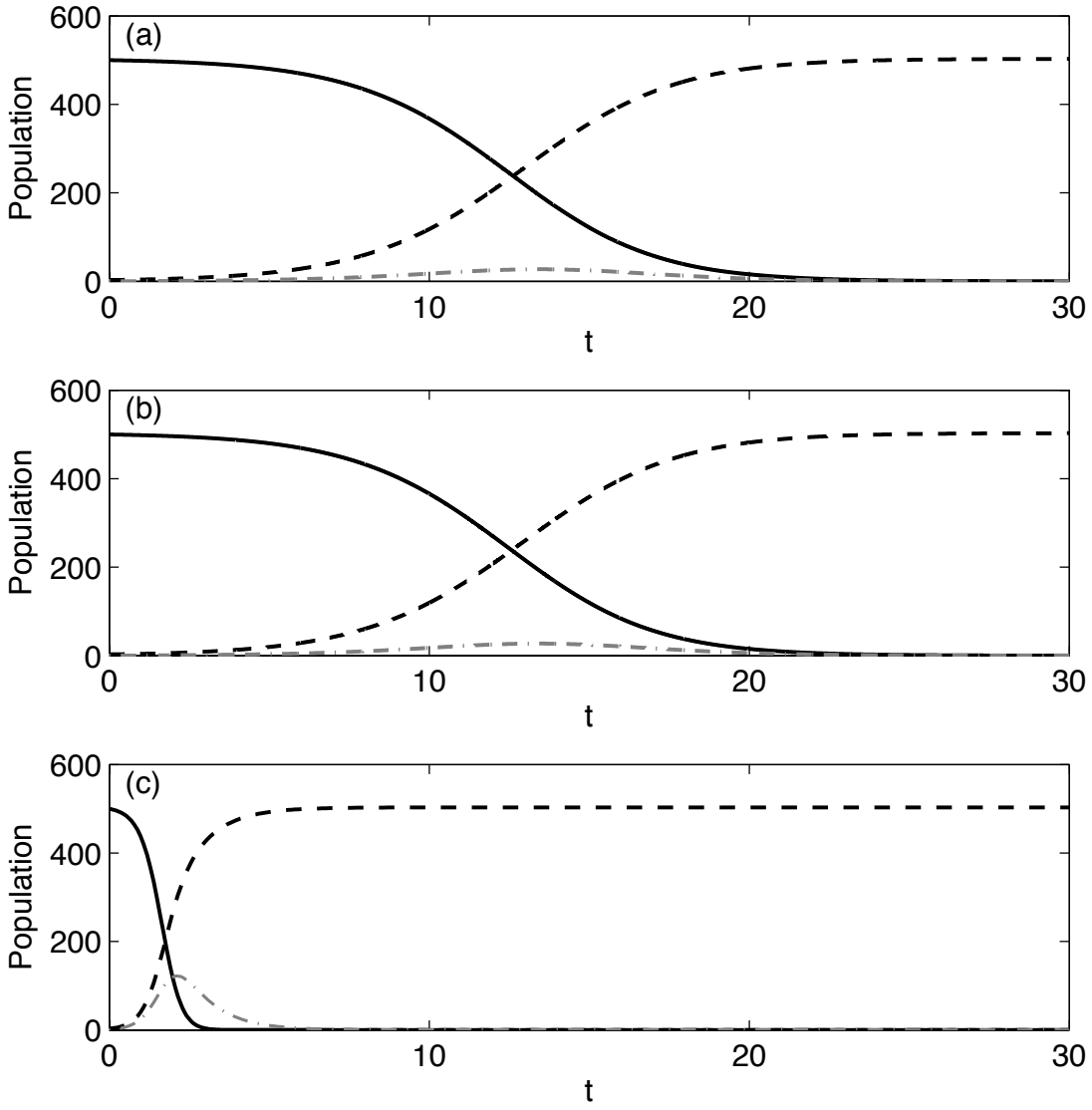

FIG. 2: **A comparison of spatial and non-spatial models.** The total susceptible (solid), zombie (dashed) and removed (dot-dashed) populations plotted as a function of time. Decay to the doomsday state (no susceptibles) is much slower for the spatial models of (a) and (b) than the non-spatial model of (c). Though the evolution of total mass in each compartment is similar for (a) and (b), the actual solution profiles are different; see Figure 3. The epidemiological parameters are $\alpha = 0.005$ and $\beta = 0.0095$ as in [1]. We begin with a total susceptible mass of 500 and a zombie mass of 3 (distributed randomly in space). (a) The full spatial model (9) with $F = 0.01$, $\ell = 0.02$, $D_S = 0.1$, $D_Z = 0.05$, and $L = 10$. (b) Like (a) but with the social interaction terms turned off, *i.e.*, $K_S = K_Z = 0$. (c) The non-spatial version of the model.

V. EPIDEMICS WITH TREATMENT

Now consider the case that there exists a treatment for zombiism. We repeat for this modified case the analytical studies presented in Section III. We perform numerical simulations

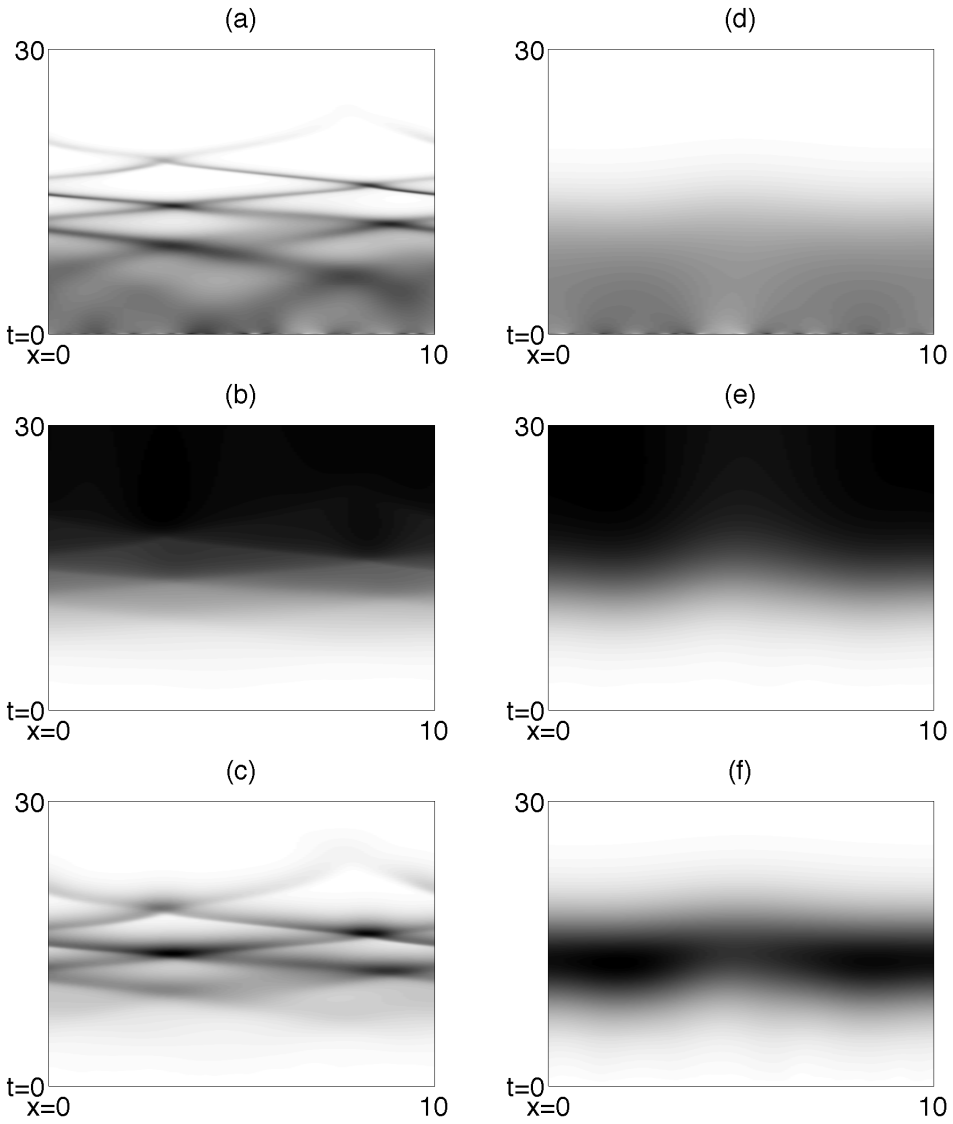

FIG. 3: **Space-time profiles of spatial models.** (a-c) S, Z, and R (respectively) for the full spatial model simulation of (9) summarized in Figure 2(a). Darker shading corresponds to higher population density. Note the presence of transient traveling pulses, which are apparent as streakiness in the picture. The system approaches the doomsday equilibrium (14). (d-f) Like (a-c), but for the diffusion-only (no social interaction) model summarized in Figure 2(b). The system approaches the same equilibrium as in (a), but transient pulses do not occur.

in the next section.

Model construction, conservation of population, and center of mass. Assume that the treatment for zombiism moves zombies back to the susceptible class with rate c.

Modifying (9) appropriately, we have

$$\dot{S} + (SK_S * Z)_x = D_S S_{xx} - \beta SZ + cZ, \tag{18a}$$

$$\dot{Z} + (ZK_Z * S)_x = D_Z Z_{xx} + \beta SZ + R - \alpha SZ - cZ, \tag{18b}$$

$$\dot{R} = \alpha SZ - R. \tag{18c}$$

This model is similar to that in Section 5 of [1] except that we do not include a class of latently-infected zombies; the introduction of treatment even without latent infection introduces new solution types into the model as we show below. Calculations identical to those of Section III establish that (18) conserves the total population size but not the center of mass.

Mass balance. We now seek mass balanced solutions. There are two different cases of mass balanced solutions for (18). The calculation of these is presented in Appendix D. The first mass balanced state is the spatially homogeneous steady state

$$(S^*, Z^*, R^*) = (N/L, 0, 0). \tag{19}$$

The second mass balanced state is actually a family of states parameterized by the quantity $\langle S, Z\rangle$, defined as

$$\langle S, Z\rangle \equiv \int_0^L SZ\, dx. \tag{20}$$

These states are

$$\int_0^L S\, dx = N - \left(\frac{\beta}{c} + \alpha\right) \langle S, Z\rangle, \tag{21a}$$

$$\int_0^L Z\, dx = \frac{\beta}{c}\langle S, Z\rangle, \tag{21b}$$

$$\int_0^L R\, dx = \alpha\langle S, Z\rangle. \tag{21c}$$

Nothing in the conditions for mass balance selects a particular member of this family. For

this family of solutions, the ratio of total members in the Z class to those in R is

$$\frac{\int_0^L Z\,dx}{\int_0^L R\,dx} = \frac{\beta}{\alpha c}. \tag{22}$$

Homogeneous steady states and stability. Eq. (18) has two spatially homogeneous steady states. One is (19) found above. The other is the endemic state

$$(S^*, Z^*, R^*) = \left(\frac{c}{\beta},\ \frac{N\beta - Lc}{L(\beta + \alpha c)},\ \frac{\alpha c}{L\beta}\frac{N\beta - Lc}{\beta + \alpha c}\right), \tag{23}$$

which exists only for

$$c/\beta < N/L. \tag{24}$$

The mass balance for (19) is

$$\int_0^L S^*\,dx = N, \quad \int_0^L Z^*\,dx = 0, \quad \int_0^L R^*\,dx = 0, \tag{25}$$

and for (23) it is

$$\int_0^L S^*\,dx = \frac{cL}{\beta}, \quad \int_0^L Z^*\,dx = \frac{N\beta - Lc}{\beta + \alpha c}, \quad \int_0^L R^*\,dx = \frac{\alpha c}{\beta}\frac{N\beta - Lc}{\beta + \alpha c}. \tag{26}$$

It is crucial to make a careful comparison between these mass balances and those of the corresponding non-spatial model. We showed in Section III that for the model without cure (9) the mass balance of steady states is the same for the spatial model as for the non-spatial model. This is *not* the case for the model with cure. The non-spatial version of the model,

$$\dot{S} = -\beta SZ + cZ, \tag{27a}$$

$$\dot{Z} = \beta SZ + R - \alpha SZ - cZ, \tag{27b}$$

$$\dot{R} = \alpha SZ - R. \tag{27c}$$

has susceptible steady state

$$(S^*, Z^*, R^*) = (N, 0, 0)\,, \tag{28}$$

which does correspond to the mass balance (25) of the susceptible state in the spatial model. However, the non-spatial model has endemic steady state

$$(S^*, Z^*, R^*) = \left(\frac{c}{\beta}, \frac{N\beta - c}{\beta + \alpha c}, \frac{\alpha c}{\beta} \frac{N\beta - c}{\beta + \alpha c} \right), \tag{29}$$

which does *not* correspond to the mass balance (26) of the endemic state in the spatial model. Thus, the introduction of spatial structure inherently shifts the mass balance of the endemic equilibrium in a manner dependent on the size of the domain.

Focusing now on steady states of the spatial model (18), we compute the linear stability of the susceptible steady state (19). The full calculation is given in Appendix F, where we derive the stability condition

$$c/\beta > N/L, \tag{30}$$

(which we have also verified numerically for sample parameters by measuring the evolution of small perturbations to the steady state). This condition is complementary to the condition (24) for existence of the endemic state.

Calculation of the linear stability of (23) is more complex. The full analysis appears in Appendix F. A primary result is that the conditions

$$\beta > \alpha, \quad D_S > 2Z^* F \ell^2, \quad \text{and} \quad D_Z > 2S^*, \tag{31}$$

are sufficient (though not necessary) for the linear stability of the endemic state. Instability of the endemic equilibrium is possible as well. For instance, the parameters

$$\begin{gathered} \alpha = 1, \quad \beta = 0.1, \quad D_S = 0.1, \quad D_Z = 0.05, \\ c = 0.2, \quad F = 0.3, \quad \ell = 0.3, \quad N = 70, \quad L = 10, \end{gathered} \tag{32}$$

provide a numerical example of instability, as demonstrated in the Appendix. For this set of parameters, note that $c/\beta = 2$ and $N/L = 7$. Hence, according to (30), the susceptible equilibrium (19) is unstable as well. Thus, we expect that the system must have long-term behavior other than a spatially homogeneous steady state. Our numerical simulations will demonstrate such behavior (see Figures 4 and 5).

In summary, we have shown that the susceptible equilibrium (19) is stable when the cure

rate c is sufficiently large as determined by (30). The endemic state (23) model can also be stable or unstable. We have demonstrated the possibility of instability via the numerical example (32) (details in Appendix F) and have derived the conditions (31) which guarantee stability for strong enough diffusion and transmission.

VI. NUMERICAL SIMULATIONS AND PERSISTENT TRAVELING PULSES

We now consider numerical results for three different models related to (18), namely the full model, the model with diffusion but no social interaction, *i.e.*, $K_S = K_Z = 0$, and the version of the model with no spatial structure. The epidemiological parameters are $\alpha = 1$, $\beta = 0.1$, and $c = 0.2$, and we take $F = 0.03$, $\ell = 0.3$, $D_S = 0.1$, $D_Z = 0.05$, and $L = 10$. We take the initial condition to satisfy

$$\int_0^L S\,dx = 50, \quad \int_0^L Z\,dx = 50, \quad R = 0, \tag{33}$$

with the nonzero populations distributed randomly in space.

Figure 4(a) shows the total number of individuals in each class S, Z, and R for the full spatial model (18). The system approaches neither a doomsday state nor an endemic steady state. Rather, the total mass in S, Z, and R fluctuate around nonzero values. In contrast to the cure-less model (9), the population of healthy humans survives. The space-time plots of Figures 5(a-c) reveal that the susceptibles survive as persistent traveling pulses that are pursued by groups of zombies. Due to the finite size of the domain and periodic boundary conditions, there is a merging and splitting of pulses, and this effect is responsible for the slight oscillation in the long-term population count in Figure 4(a).

Figures 4(b) and 5(a-c) correspond to the reduced spatial model without social interaction. In this case, the system reaches the spatially homogeneous endemic equilibrium with mass balance (26). While some healthy, alert humans survive, their total mass is less than that contained in the traveling pulse of susceptibles discussed above. Hence, for at least some parameters, social effects can enhance the survival of the healthy human population.

Figure 4(c) corresponds to the compartmental model (27). The system again reaches an endemic equilibrium, albeit with different levels of S, Z, and R. As discussed above, the mass balance (26) for the endemic equilibrium within the spatial model necessarily differs

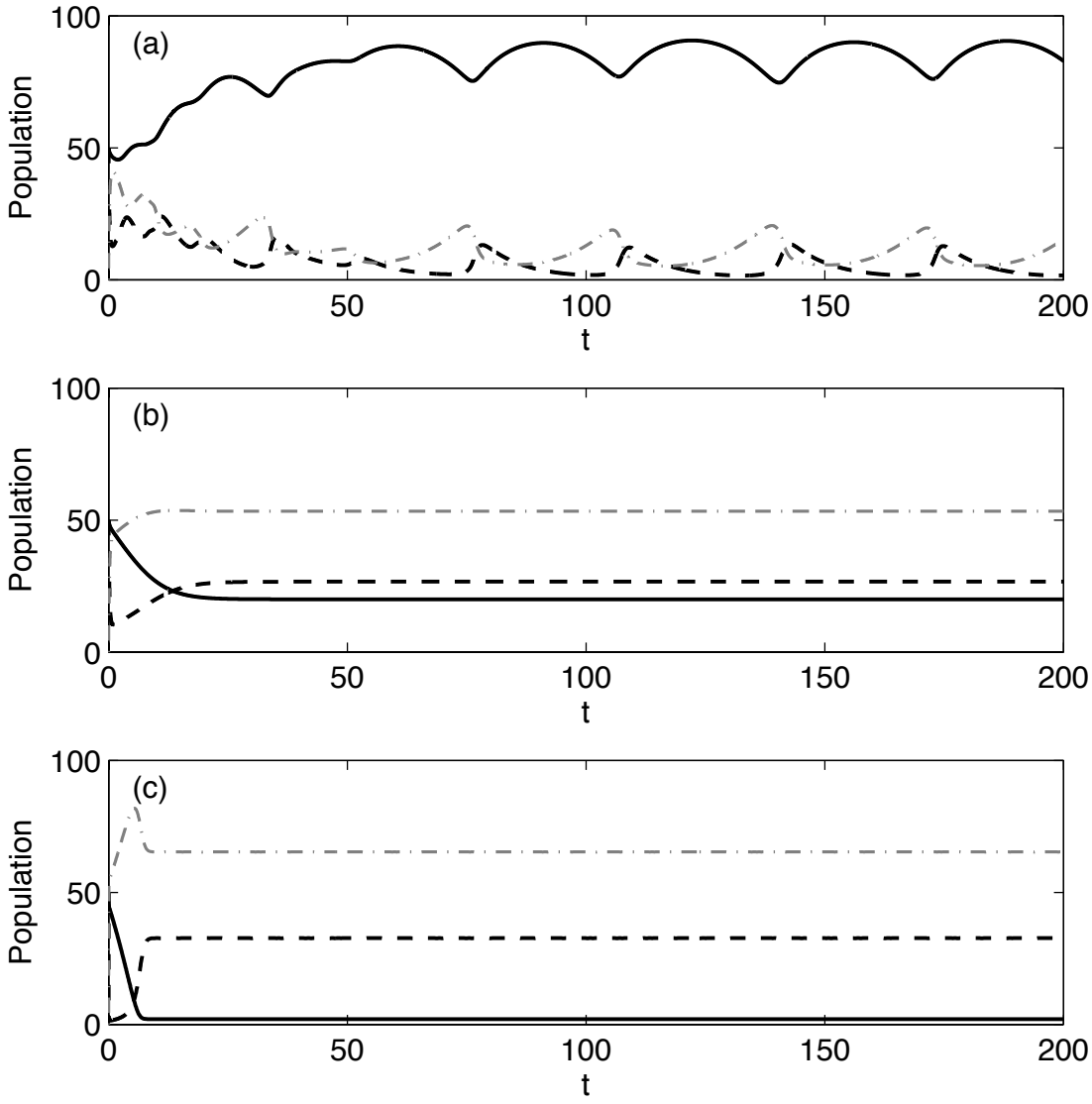

FIG. 4: **A comparison of spatial and non-spatial models with a zombie cure.** The total susceptible (solid), zombie (dashed) and removed (dot-dashed) populations plotted as a function of time for $\alpha = 1$, $\beta = 0.1$, $c = 0.2$ and an initial condition of 50 susceptibles and 50 zombies. (a) The full model (18) produces a persistent susceptible population. Here, $F = 0.03$, $\ell = 0.3$, $D_S = 0.1$, $D_Z = 0.05$, and $L = 10$. (b) The reduced model (18) with no social forces, *i.e.*, $K_S = K_Z = 0$, reaches the endemic equilibrium with mass balance (26). Asymptotically, more susceptibles survive for the case shown in (a) with social advection. (c) The compartmental model reaches an endemic equilibrium with mass balance (29), in which even fewer susceptibles survive.

from the mass balance (29) for the compartmental model.

For the full model (18), the splitting and merging pulses are not the only long-term behavior we have observed. We have conducted simulations at different parameter values, revealing slightly different non-steady-state solutions. To systematize our study, we fix the

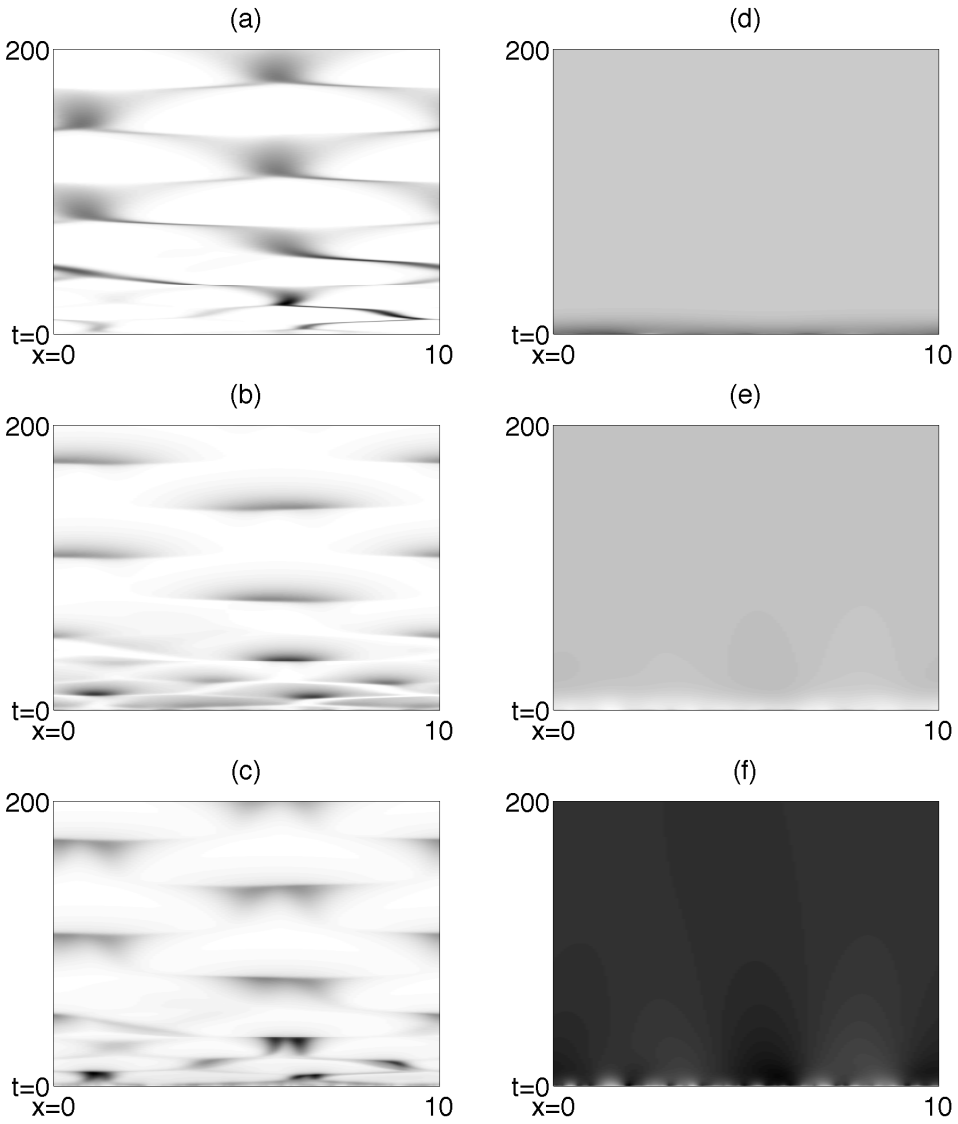

FIG. 5: **Space-time profiles of spatial models with zombie cure.** (a-c) S, Z, and R (respectively) for the full spatial model simulation summarized in Figure 4(a). Darker shading corresponds to higher population density. Note the presence of splitting and merging traveling pulses. (d-f) Like (a-c), but for the diffusion-only (no social interaction) model summarized in Figure 4(b). Pulses do not occur, and the system reaches the spatially homogeneous steady state (23).

following parameters to the values in Figures 4 and 5: $\alpha = 1$, $\beta = 0.1$, $\ell = 0.3$, $D_S = 0.1$, $D_Z = 0.05$, and $L = 10$. We concentrate on the dependence of the solutions on c and F in the range $0 \leq c \leq 0.21$ and $0.01 \leq F \leq 0.05$. (This range is chosen based on preliminary studies on a larger parameter range. For c much larger, the susceptible steady state attracts all of the initial conditions that we tried.) We run each simulation to time $t = 60$ to remove transient behavior. We then retain the data from $t = 60$ to 120 for study. Our findings are

F	0.01	0.014	0.019	0.023	0.28	0.032	0.037	0.041	0.046	0.05
c										
0.01	Transient Pulses									
0.03	2.43	2.41	2.26	2.30	2.15	2.13	−2.10	2.12	2.04	−1.97
0.05	2.72	−2.30	−2.75	−2.13	2.08	−2.57	1.99	1.94	1.89	1.87
0.08	3.13	3.07	−3.09	2.28	−2.35	2.19	−2.41	−2.08	−2.14	−2.07
0.10	−3.84	−2.80	2.47	2.62	3.60	−2.41	3.19	−2.72	−2.37	2.41
0.12	−3.23	−3.10	3.09	−2.76	−3.14	2.85	−2.71	−2.83	−2.71	HC
0.14	4.76 P	3.73	HC	−4.04 P	3.71	3.76 P	3.76 P	−3.15	−3.21	3.38
0.17	−4.36	HC	−4.75	4.01	−4.06	−4.05	4.04	4.39 P	4.36 P	−4.25
0.19	5.02 P	HC	HC	HC	−4.58 PP	−5.02 PP	4.48	4.82 P	−4.77 P	4.19 P
0.21	5.17 PP	HC	HC	4.92 P	HC	−5.80 PP	5.48 PP	−5.38 PP	HC	HC

TABLE I: **Non-steady-state attracting solutions and their velocity for the spatial model with zombie cure.** This table summarizes the type of solutions found in simulations of (18) for varying c and F values in the range $0 \leq c \leq 0.21$ and $0.01 \leq F \leq 0.05$ where we have fixed $\alpha = 1, \beta = 0.1, \ell = 0.3, D_S = 0.1, D_Z = 0.05$ and $L = 10$. The initial conditions have total mass of the S and Z populations both equal to 50, distributed randomly in space. We have performed one simulation per parameter value. If the solution is a traveling pulse, its velocity is stated. Oscillatory and highly oscillatory traveling pulses are denoted with a P and a PP respectively after the value of the average velocity. Finally, HC denotes solutions in which pulses periodically split and rejoin, giving a honeycomb-like appearance to the space-time diagram. A velocity no longer makes sense for such solutions.

summarized in Table I.

We find three distinct long-term behaviors that are not spatially homogeneous steady states. For c slightly greater than zero, there are traveling pulse solutions with constant velocity; Figure 6(a-c) shows an example. These types of solutions are indicated in the Table by entries consisting only of a numerical entry, which is the traveling velocity of the pulse. The speed depends on the c and F, but the simulations indicate that the direction is dependent only on the initial conditions (which is consistent with the equations themselves having no inherent direction preference). As c grows larger, the velocity increases. For larger c values, the solutions still are traveling pulses, but with accompanying oscillation in the pulse speed; Figure 6(d-f) shows an example. These solutions are indicated in the Table by entries marked with a P or PP (to denote low or high degrees of oscillation). The number given is the average velocity, which generally appears to be close to the speed of non-oscillating pulses nearby in parameter space. Finally, for certain large c values, pulses periodically join and split. We have already shown this type of solution in Figure 5(a-c) and we give an additional example in Figure 6(g-i) for comparison with the other solution types.

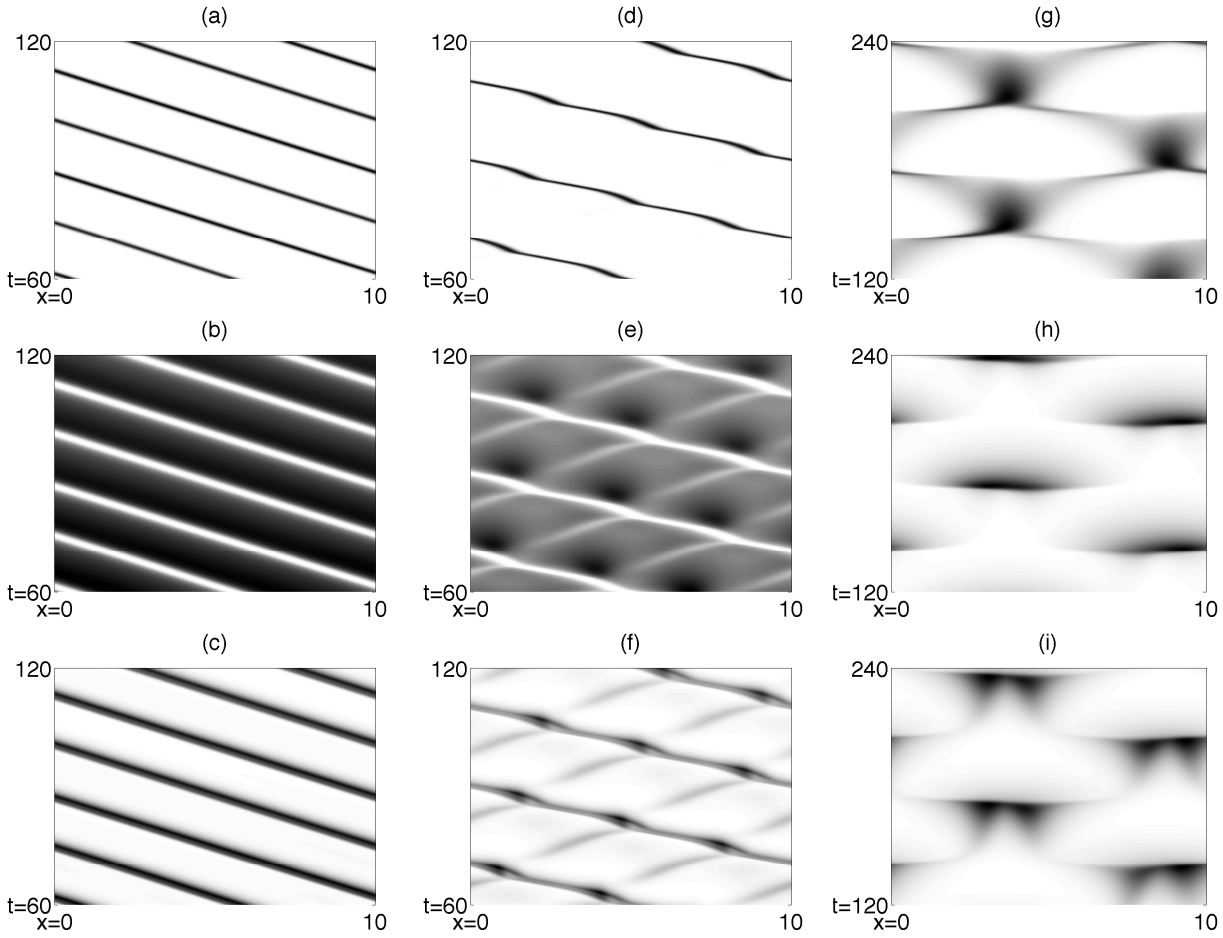

FIG. 6: **Different persistent traveling solutions in the case of a zombie cure.** Space-time diagrams of susceptibles S (top), zombies Z (middle), and recovereds R (bottom) in simulations of (18) with $\alpha = 1$, $\beta = 0.1$, $\ell = 0.3$, $D_S = 0.1$, $D_Z = 0.05$, $L = 10$, and initial conditions of 50 susceptibles and 50 zombies distributed randomly in space. For all figures, we show only the latter portion of the simulation to eliminate any transients. (a-c) A traveling pulse with constant velocity, for $c = 0.054$ and $F = 0.032$. (d-f) A traveling pulse with oscillating velocity, for $c = 0.054$ and $F = 0.037$. (g-i) Merging and splitting pulses, for $c = 0.21$ and $F = 0.046$.

The solutions looks much like a honeycomb in space-time, and we have marked them as HC in the Table.

It is theoretically possible that at certain parameter values, there could be coexisting stable solutions. In fact, based on preliminary numerical experiments, we anticipate that for the larger c values for which we start seeing oscillatory pulses and merging/splitting pulses, the individual pattern selection (*i.e.*, long term behavior of splitting/merging pulses versus oscillatory pulse) depends only on the initial condition, and this dependence is likely responsible for the nonmonotonic dependence of solution type on the parameters c and F

in the Table.

VII. CONCLUSION

In this paper, we have considered spatial models of zombie epidemics. Our model is based on that in [1]. The spatial elements we introduce capture social forces between zombies and alert, healthy humans. In particular, we have incorporated the tendency of healthy humans to move away from zombies, and the tendency of zombies to move towards healthy humans.

For our spatial model (9), the main analytical results include:

- We show explicitly that the center of mass of the population may travel.
- Mass balanced solutions have no removed individuals. They have spatial separation between zombies and susceptibles.
- The only steady possible state solutions are the spatially homogeneous susceptible and doomsday states.
- The susceptible state is linearly unstable, and the doomsday state is linearly stable.

Numerical simulations provided further information. For the non-spatial version of the model in [1], the only stable equilibrium is the doomsday state in which all individuals are zombies. In the spatial model, not only is this state linearly stable, but it is also the only long-term behavior observed in numerical simulations. However, in the spatial model, convergence to the equilibrium can occur more slowly than in the non-spatial model, and this convergence occurs via a self-organized cluster of susceptibles that is pursued by a group of zombies. The additional time to the annihilation of alert humans might allow for the development of a cure.

In this vein, we considered a modification of our spatial model to include a cure for zombiism. Results for (18) include:

- Mass balanced solutions do not necessarily have spatial separation between zombies and susceptibles.
- The model has two spatially homogeneous steady states. One is the susceptible state, which has the same mass balance as the susceptible state in the non-spatial analogue

of the model. The other is the endemic state. The mass balance of the endemic state differs from that of the endemic state in the non-spatial model.

- The susceptible steady state exists for all parameter values, and is linearly stable for a sufficiently large cure rate.
- The endemic steady state exists for a sufficiently small cure rate, and is stable if diffusion and transmission are sufficiently large.
- There exist parameter regimes in which both homogeneous steady states are unstable.

Via numerical simulations, we saw the existence of three qualitatively distinct types of solutions that are not homogeneous steady states. Each consisted of self-organized pulses of healthy, alert humans pursued by groups of zombies. In the first type, the pulse travels at constant velocity. In the second, the pulse travels at a nonzero average velocity, but is oscillatory. In the third type, there is a periodic splitting and rejoining of the susceptible population. In contrast to the first model (9) in which a cure was absent, these traveling pulses of susceptibles in (18) are all persistent, signaling hope of survival for the healthy population. Furthermore, in many of our example simulations, the total mass contained in the susceptible pulse was greater than that of the susceptibles within the spatially homogeneous endemic equilibrium.

We close with some open questions for the community of mathematicians undertaking zombie research. We show in Appendix E that homogeneous steady states are the only steady states of (9). However, this argument assumes continuity of the functions S and Z. A proof of regularity of the solutions is needed to justify this assumption. On a related topic, our numerics indicate that homogeneous steady states are not just the only steady states, but are the only mass balanced states; however, a proof of this statement is lacking. In addition, one could imagine attractors that are not steady states, and are not mass balanced, but perhaps are time-periodic. Based on the variety of numerical simulations we have conducted, we conjecture that the doomsday state is the only attractor, but a definitive proof is lacking. Such a proof would also serve, among other things, to rule out the possibility of persistent traveling pulses for this model.

For the model (18) with a cure we have shown analytically that depending on parameter choices, there is a susceptible steady state and an endemic steady state in which zombies

and alert humans coexist. Our numerical simulations indicate that there exist attractors other than homogeneous steady states. In fact, we observed three different types of traveling pulses. We pose as an open problem the analytical proof for the existence of traveling pulses. Numerical simulations also indicate that bi-stability of the different types of solutions is possible. There is a need for more extensive numerical examination of these coexisting pulse types, followed by the development of early detection methods to distinguish between them. The early detection methods are of high priority, since they would allow more time for the implementation of the distinct corresponding strategies which would be needed for surviving a zombie epidemic.

Appendix A: Nondimensionalization

To reduce the number of parameters in the original dimensioned model (8), we nondimensionalize as follows. Let

$$x \rightarrow \ell_S \hat{x}, \tag{A1a}$$

$$t \rightarrow \frac{1}{\zeta}\hat{t}, \tag{A1b}$$

$$\{S, Z, R\} \rightarrow \frac{\ell_S \zeta}{F_S}\{\hat{S}, \hat{Z}, \hat{R}\}. \tag{A1c}$$

Substituting, cleaning up, and dropping the hats, we have

$$\dot{S} + \left(S\left\{\mathrm{sgn}(x)\cdot e^{-|x|} * Z\right\}\right)_x = \frac{D_S}{\ell_S^2\zeta}S_{xx} - \frac{\beta\ell_S}{F_S}SZ, \tag{A2a}$$

$$\dot{Z} + \left(Z\left\{-\mathrm{sgn}(x)\cdot F_Z/F_S e^{-|x|\ell_S/\ell_Z} * S\right\}\right)_x = \frac{D_Z}{\ell_S^2\zeta}Z_{xx} - \frac{\beta\ell_S}{F_S}SZ + R - \frac{\alpha\ell_S}{F_S}SZ, \tag{A2b}$$

$$\dot{R} = -\frac{\alpha\ell_S}{F_S}SZ - R, \tag{A2c}$$

where the overdot and the subscript x are now understood to represent derivatives with respect to dimensionless variables. Now define

$$F = F_Z/F_S, \tag{A3a}$$

$$\ell = \ell_Z/\ell_S. \tag{A3b}$$

For convenience, redefine

$$K_S = \mathrm{sgn}(x) \cdot e^{-|x|}, \tag{A4a}$$

$$K_Z = -\mathrm{sgn}(x) \cdot F e^{-|x|/\ell}, \tag{A4b}$$

and

$$\frac{\alpha \ell_S}{F_S} \to \alpha, \tag{A5a}$$

$$\frac{\beta \ell_S}{F_S} \to \beta, \tag{A5b}$$

$$\frac{D_S}{\ell_S^2 \zeta} \to D_S, \tag{A5c}$$

$$\frac{D_Z}{\ell_S^2 \zeta} \to D_Z. \tag{A5d}$$

Then the model reads

$$\dot{S} + (SK_S * Z)_x = D_S S_{xx} - \beta SZ, \tag{A6a}$$

$$\dot{Z} + (ZK_Z * S)_x = D_Z Z_{xx} + \beta SZ + R - \alpha SZ, \tag{A6b}$$

$$\dot{R} = \alpha SZ - R, \tag{A6c}$$

which is (9). Here, K_S and K_Z are given by (A4). The dimensionless parameters $F \leq 1$ and $\ell \leq 1$ measure, respectively, the relative strength and length scale of attraction to repulsion. The parameters D_S, D_Z, α, and β are dimensionless versions of the corresponding parameters in the original dimensioned model.

Appendix B: Conservation of population

Here we show that the total population size remains constant under the dynamics of (9). First we add the three equations in (9) together, rearrange, and expand spatial derivatives to obtain

$$\frac{\partial}{\partial t}(S + Z + R) = D_S S_{xx} + D_Z Z_{xx} - (SK_S * Z)_x - (ZK_Z * S)_x. \tag{B1}$$

Now integrate over the domain $[0, L]$ and assume that this operation commutes with time differentiation. We recall the definitions (11) and we also define the inner product on two

functions a and b as

$$\langle a, b\rangle \equiv \int_0^L a \cdot b \, dx. \tag{B2}$$

Then (B1) is

$$\dot{N} \;=\; D_S\langle S_{xx}, 1\rangle + D_Z\langle Z_{xx}, 1\rangle - \langle (SK_S * Z)_x, 1\rangle - \langle ZK_Z * S, 1\rangle. \tag{B3}$$

Using integration by parts, and recalling that the convolution of two L-periodic functions is L-periodic, we have

$$\langle S_{xx}, 1\rangle \;=\; S_x(L) - S_x(0) = 0, \text{ and} \tag{B4}$$

$$\langle (SK_S * Z)_x, 1\rangle \;=\; S(L)(K_S * Z)(L) - S(0)(S_S * Z)(0) = 0. \tag{B5}$$

Similar statements hold for the Z terms. Hence,

$$\dot{N} = 0,$$

and the total population is conserved, as with the compartmental model from [1]. The calculation showing conservation of mass for (18) is essentially identical.

Appendix C: Center of mass

In this appendix we show that the population center of mass is not conserved under (9), and we derive a time-dependent upper bound on the speed at which the center of mass can travel.

Begin with the first moment $\langle n, x\rangle$ of $n(x,t)$ (proportional to the center of mass) by

taking an inner product of $\dot{n}$ with x. We obtain

$$\begin{aligned}
\langle \dot{n}, x\rangle &= D_S\langle S_{xx}, x\rangle + D_Z\langle Z_{xx}, x\rangle && \text{(C1a)}\\
&\quad -\langle (SK_S * Z)_x, x\rangle - \langle (ZK_Z * S)_x, x\rangle,\\
&= H(t) + \langle SK_S * Z, 1\rangle + \langle ZK_Z * S, 1\rangle, && \text{(C1b)}\\
&= H(t) + \langle S, K_S * Z\rangle + \langle K_Z * S, Z\rangle, && \text{(C1c)}\\
&= H(t) + \langle S, K_S * Z\rangle + \langle S, K_Z * Z\rangle, && \text{(C1d)}\\
&= H(t) + \langle S, K * Z\rangle, && \text{(C1e)}
\end{aligned}$$

where $K = K_S + K_Z$, and $H(t) = L(D_s S_x(L,t) + D_z Z_x(L,x) - (Sv_s(L,t) + Zv_z(L,t)))$. The second equation follows from integration by parts (twice for the diffusive terms and once for the advective ones), the third follows from properties of multiplication, and the fourth follows from the fact that convolution may be moved across the inner product. In the integration by parts leading to the second equation, note that the boundary terms which would arise all collapse to $H(t)$ due to the periodic boundary conditions. Since the quantity in (C1e) is generically nonzero, it follows that the center of mass of the solution is not conserved, which means traveling solutions are not *a priori* ruled out, although in our numerical simulations of (9) we have only found transient traveling solutions; see Figures 2(a) and 3(a-c).

Using our previous calculation, we can bound the speed at which the center of mass of n (equivalently, the first moment divided by the total mass) is permitted to move. Define $x_c(t) = \langle n, x\rangle/N$, the center of mass of n. Let $G(t) = H(t)/N$. From our calculation above,

$$\begin{aligned}
|\dot{x}_c| &= |\langle S, K * Z\rangle|/N + G(t), && \text{(C2a)}\\
&\leq \langle S, |K| * Z\rangle/N + G(t), && \text{(C2b)}\\
&= \||S|K| * Z\|_1/N + G(t), && \text{(C2c)}\\
&\leq \|S\|_1 \cdot \||K| * Z\|_\infty/N + G(t), && \text{(C2d)}\\
&\leq \|S\|_1 \cdot \|K\|_\infty \cdot \|Z\|_1/N + G(t), && \text{(C2e)}\\
&\leq \frac{1}{4}\|K\|_\infty N^2/N + G(t), && \text{(C2f)}\\
&\leq \frac{1}{4}\|K\|_\infty N + G(t), && \text{(C2g)}
\end{aligned}$$

where the second line follows from the property of absolute value, the third from the defini-

tion of the L^1 norm, the fourth from Hölder's inequality, the fifth from Young's inequality for convolutions, and the sixth from the fact that $\|S\|_1 + \|Z\|_1 \leq N$ and so the maximum value of $\|S\|_1 \cdot \|Z\|_1$ is $N^2/4$. Therefore,

$$\frac{1}{4}\|K\|_\infty N + G(t), \tag{C3}$$

is an upper bound on the speed of the center of mass of the population.

We can find $\|K\|_\infty$ using simple calculus. From the antisymmetry of K, it suffices to consider K on $x \geq 0$, where $K \geq 0$. The global maximum on this domain must either occur at $x = 0$ or at the critical point where $K' = 0$. The critical point is

$$x_{crit} = \frac{\ell \ln(\ell/F)}{\ell - 1}. \tag{C4}$$

If $F < \ell$ then the critical point is outside of the domain. The global maximum, therefore, is $K(0) = 1 - F$. If $F = \ell$ then the critical point coincides with the domain boundary and $1 - F$ is still the global maximum. On the other hand, if $F \geq \ell$, the critical point is on the interior of the domain, and the global maximum is $K(x_{crit})$. In summary, we have

$$\|K\|_\infty = \begin{cases} 1 - F & F \leq \ell, \\ \left(\frac{\ell}{F}\right)^{\frac{\ell}{1-\ell}} - F\left(\frac{\ell}{F}\right)^{\frac{1}{1-\ell}} & F > \ell, \end{cases} \tag{C5}$$

where in the bottom expression we have evaluated $K(x_{crit})$.

Note that as $F, \ell \to 1$, the upper bound (C3) implies that the maximum speed of a traveling solution limits to $L/N(D_s S_x(L,t) + D_z Z_x(L,t))$.

For the cure model (18), the demonstration that center of mass is not conserved and the bound for the speed of the center of mass are essentially identical to what we have presented in this appendix.

Appendix D: Mass balanced states

We seek mass balanced states of (9), that is, states where the number of individuals within each class is not changing in time, even if the solution profiles themselves are. We

integrate each of (9) on the real line to obtain

$$\begin{aligned}
\langle \dot{S}, 1\rangle + \langle (SK_S * Z)_x, 1\rangle &= \langle D_S S_{xx}, 1\rangle - \langle \beta SZ, 1\rangle, && \text{(D1a)}\\
\langle \dot{Z}, 1\rangle + \langle (ZK_Z * S)_x, 1\rangle &= \langle D_Z Z_{xx}, 1\rangle + \langle \beta SZ, 1\rangle && \text{(D1b)}\\
&\quad + \langle R, 1\rangle - \langle \alpha SZ, 1\rangle,\\
\langle \dot{R}, 1\rangle &= \langle \alpha SZ, 1\rangle - \langle R, 1\rangle. && \text{(D1c)}
\end{aligned}$$

At mass balance, the first term of each equation will be zero by definition. Using integration by parts shows terms involving spatial derivatives are zero. Then (D1) simplifies to

$$\begin{aligned}
\langle S, Z\rangle &= 0, && \text{(D2a)}\\
(\beta - \alpha)\langle S, Z\rangle + \langle R, 1\rangle &= 0, && \text{(D2b)}\\
\alpha\langle S, Z\rangle - \langle R, 1\rangle &= 0. && \text{(D2c)}
\end{aligned}$$

Substituting (D2a) into (D2c) shows that R must be identically zero. Eq. (D2a) itself implies that in a point-wise sense, either S or Z is 0. Thus, at mass balance (and therefore, at any steady states) there is physical separation between susceptibles and zombies. They cannot coexist at the same spatial location.

We now consider mass balanced states of (18). The conditions (D2) are modified to

$$\begin{aligned}
-\beta\langle S, Z\rangle + c\langle Z, 1\rangle &= 0, && \text{(D3a)}\\
(\beta - \alpha)\langle S, Z\rangle + \langle R, 1\rangle - c\langle Z, 1\rangle &= 0, && \text{(D3b)}\\
\alpha\langle S, Z\rangle - \langle R, 1\rangle &= 0. && \text{(D3c)}
\end{aligned}$$

The solution may be written in terms of $\langle S, Z\rangle$ as

$$\begin{aligned}
\int_0^L S\,dx &= N - \left(\frac{\beta}{c} + \alpha\right)\langle S, Z\rangle, && \text{(D4a)}\\
\int_0^L Z\,dx &= \frac{\beta}{c}\langle S, Z\rangle, && \text{(D4b)}\\
\int_0^L R\,dx &= \alpha\langle S, Z\rangle. && \text{(D4c)}
\end{aligned}$$

We consider separately two cases for $\langle S, Z\rangle$. If $\langle S, Z\rangle = 0$ then the only mass balanced state

is the spatially homogeneous steady state (19). If $\langle S, Z\rangle \neq 0$ then there is a family of mass balanced states parameterized by $\langle S, Z\rangle$, as discussed in Section V.

Appendix E: Steady states of (9)

We show that the only possible steady states of (9) are spatially homogeneous. The steady state problem corresponding to (9) is

$$(SK_S * Z)_x = D_S S_{xx} - \beta SZ, \tag{E1a}$$

$$(ZK_Z * S)_x = D_Z Z_{xx} + \beta SZ + R - \alpha SZ, \tag{E1b}$$

$$0 = \alpha SZ - R. \tag{E1c}$$

Since steady states are automatically mass balanced states, we know from Appendix D that R is identically zero, and the product SZ is identically zero.

Assume that $Z(a) \neq 0$ for some $a \in [0, L]$, and assume further that Z is continuous. We now show that the solution is a spatially homogeneous steady state. By the continuity of Z, $Z \neq 0$ in a neighborhood of a. By the fact that $SZ = 0$, $S(x) = S_x(x) = 0$ in this neighborhood. By (E1),

$$(SK_S * Z)_x = D_S S_{xx}. \tag{E2}$$

Integrating from a to x, we get

$$S_x = \left(\frac{K_S * Z}{D_S}\right) S. \tag{E3}$$

The solution to this equation is

$$S(x) = S(a)\ exp\left(\frac{\int_a^x K_S * Z\ ds}{D_S}\right) \equiv 0. \tag{E4}$$

Therefore we have shown that the solution is an spatially homogeneous steady state solution. A similar calculation shows that if $S(a) \neq 0$, then $Z \equiv 0$.

Thus, the only steady states are spatially homogeneous ones, namely (13) and (14).

Appendix F: Linear stability

We compute the linear stability of the steady states (13) and (14) of (9) by allowing small perturbations, which for convenience we write in a normal mode expansion, that is,

$$S = S^* + \sum_k S_k(t)e^{ikx}, \quad Z = Z^* + \sum_k Z_k(t)e^{ikx}, \quad R = R^* + \sum_k R_k(t)e^{ikx}, \tag{F1}$$

where the wave number k is

$$k = \frac{2j\pi}{L}, \quad j \in \mathbb{Z}, \tag{F2}$$

to be commensurate with the periodic domain.

In the analysis below, since the ranges of K_S and K_Z are small compared to the size of the domain (*i.e.*, $L \gg 1$), we approximate the Fourier transforms of the repulsive and attractive kernels by their values on the infinite domain:

$$\widehat{K}_S(k) \approx -\frac{2ik}{1+k^2}, \tag{F3a}$$

$$\widehat{K}_Z(k) \approx \frac{2iF\ell^2 k}{1+\ell^2 k^2}. \tag{F3b}$$

$$\tag{F3c}$$

Let $U_k = (S_k, Z_k, R_k)^T$. We substitute (13) and (14) into a linearized version of (9), giving us the system

$$\frac{d}{dt}U_k = \mathbf{L}U_k, \tag{F4}$$

where $\mathbf{L}$ consists of terms arising from advection, diffusion, and the original compartmental model of [1]:

$$\mathbf{L} = \mathbf{L}_{adv} + \mathbf{L}_{diff} + \mathbf{L}_{comp}. \tag{F5}$$

We have

$$\mathbf{L}_{comp} = \begin{pmatrix} -\beta Z^* & -\beta S^* & 0 \\ (\beta-\alpha)Z^* & (\beta-\alpha)S^* & 1 \\ \alpha Z^* & \alpha S^* & -1 \end{pmatrix}, \tag{F6}$$

and

$$\mathbf{L}_{diff} = \begin{pmatrix} -D_S k^2 & 0 & 0 \\ 0 & -D_Z k^2 & 0 \\ 0 & 0 & 0 \end{pmatrix}. \tag{F7}$$

For the linearized advection operator, we have

$$\mathbf{L}_{adv} = \begin{pmatrix} 0 & -ik\widehat{K}_S(k)S^* & 0 \\ -ik\widehat{K}_Z(k)Z^* & 0 & 0 \\ 0 & 0 & 0 \end{pmatrix}, \tag{F8}$$

but use (F3) to write

$$\mathbf{L}_{adv} \approx \begin{pmatrix} 0 & -\dfrac{2k^2}{1+k^2}S^* & 0 \\ \dfrac{2F\ell^2k^2}{1+\ell^2k^2}Z^* & 0 & 0 \\ 0 & 0 & 0 \end{pmatrix}. \tag{F9}$$

In obtaining the expression (F8) we have used the fact that x derivatives transform as ik and convolution with a kernel K transforms as multiplication by $\widehat{K}$.

Using this general form of the linearization, we can analyze stability for each of the steady state solutions.

For (13), the linearization is

$$\mathbf{L} = \begin{pmatrix} -D_S k^2 & -\dfrac{2(N/L)k^2}{1+k^2} - \beta N/L & 0 \\ 0 & -D_Z k^2 + (\beta - \alpha)N/L & 1 \\ 0 & \alpha N/L & -1 \end{pmatrix}. \tag{F10}$$

Linear (in)stability will depend on the eigenvalues of the matrix $\mathbf{L}$. Though the eigenvalues may be computed directly, the expressions are inconvenient to analyze. Instead, recall that the characteristic polynomial may be written down in terms of the eigenvalues $\lambda_{1,2,3}$ as

$$\lambda^3 - \tau\lambda^2 + \gamma\lambda - \Delta = 0, \tag{F11}$$

where

$$\tau = \text{trace} \qquad = \lambda_1 + \lambda_2 + \lambda_3, \tag{F12a}$$

$$\gamma = \text{cross terms} \;= \lambda_1\lambda_2 + \lambda_1\lambda_3 + \lambda_2\lambda_3, \tag{F12b}$$

$$\Delta = \text{determinant} = \lambda_1\lambda_2\lambda_3. \tag{F12c}$$

From (F4) it follows that

$$\tau(k) \;=\; -(D_S + D_Z)k^2 + (\beta - \alpha)N/L - 1, \tag{F13a}$$

$$\gamma(k) \;=\; D_S D_Z k^4 + \left[D_S(\alpha - \beta)N/L + D_S + D_Z\right] k^2 - \beta N/L, \tag{F13b}$$

$$\Delta(k) \;=\; -D_S D_Z k^4 + (D_S \beta N/L)k^2. \tag{F13c}$$

For the equilibrium to be linearly stable, the eigenvalues $\lambda_{1,2,3}(k)$ must have negative real part for all admissible k. It follows from (F12) that necessary conditions are $\tau < 0$, $\gamma > 0$, $\Delta < 0$ for all k. An examination of (F13) shows that it is impossible to satisfy these necessary conditions. For instance, the opposing signs on the k^2 and k^4 terms in $\Delta(k)$ mean that $\Delta > 0$ for some k, and hence the equilibrium is linearly unstable as long to generic noisy perturbations as L is sufficiently large. This result of linear instability is the same as for the non-spatial model in [1].

For the susceptible equilibrium (13), the linear stability matrix is

$$\mathbf{L} = \begin{pmatrix} -D_S k^2 - \beta N/L & 0 & 0 \\ \dfrac{2NF\ell^2 k^2}{1+\ell^2 k^2} + (\beta - \alpha)N/L & -D_Z k^2 & 1 \\ \alpha N/L & 0 & -1 \end{pmatrix} \tag{F14}$$

which has eigenvalues with simple expressions that are easy to analyze. We have

$$\lambda_1 = -D_S k^2 - \beta N/L, \quad \lambda_2 = -D_Z k^2, \quad \lambda_3 = -1. \tag{F15}$$

Since $\lambda_{1,2,3} < 0$, we see that the population is linearly stable, as in the non-spatial model. The only exception is for a perturbation with $k = 0$, in which case there is one eigenvalue equal to zero. The corresponding eigenvector is $(S_0, Z_0, R_0) = (0, 1, 0)$ which tells us that a

perturbation that changes an all-zombie state to another all-zombie state (by changing the total population size) is neutrally stable.

We now turn attention to the linear stability of homogeneous steady states of the cure model (18). The calculation is similar to those presented above. Stability of the susceptible equilibrium (19) is determined by the matrix

$$\mathbf{L} = \begin{pmatrix} -D_S k^2 & -\dfrac{2(N/L)k^2}{1+k^2} - \beta N/L + c & 0 \\ 0 & -D_Z k^2 + (\beta - \alpha)N/L - c & 1 \\ 0 & \alpha N/L & -1 \end{pmatrix}. \tag{F16}$$

One eigenvalue has a simple expression, $\lambda_1 = -D_S k^2 \leq 0$. It follows from above that the remaining eigenvalues satisfy

$$\lambda_2 + \lambda_3 = -D_Z k^2 + (\beta - \alpha)N/L - 1 - c, \tag{F17a}$$

$$\lambda_2 \lambda_3 = D_Z k^2 - \beta N/L + c. \tag{F17b}$$

Necessary and sufficient conditions for the remaining two eigenvalues to have negative real part are $\lambda_2 + \lambda_3 \leq 0$ and $\lambda_2 \lambda_3 \geq 0$ which lead to the stability condition (30).

The linear stability of the endemic state (23) is determined by the matrix

$$\mathbf{L} = \begin{pmatrix} -D_S k^2 - \beta Z^* & -\dfrac{2S^* k^2}{1+k^2} & 0 \\ \dfrac{2Z^* F \ell^2 k^2}{1+\ell^2 k^2} + (\beta - \alpha)Z^* & -D_Z k^2 - \alpha S^* & 1 \\ \alpha Z^* & \alpha S^* & -1 \end{pmatrix}, \tag{F18}$$

where we have used the equilibrium value for S^* to simplify parts of some entries in the matrix in order to have convenient expressions. It is straightforward to compute eigenvalues of (F18) numerically. We also make some analytical statements. Recall from (F12) that necessary conditions for stability are $\tau < 0$, $\gamma > 0$, $\Delta < 0$ for all k. For (F18),

$$\tau(k) = -(D_S + D_Z)k^2 - 1 - Z^*\beta - \frac{\alpha c}{\beta} < 0, \tag{F19a}$$

$$\Delta(k) = -D_Z k^2 \left(\beta Z^* + D_S k^2\right) - \frac{2cZ^* k^2}{1+k^2} - \frac{4F\ell^2 cZ^* k^4}{\beta\left(1+\ell^2 k^2\right)\left(1+k^2\right)} \leq 0, \tag{F19b}$$

with $\Delta(k) = 0$ only for $k = 0$. However, the lengthy expression for γ (omitted here) is of indeterminate sign. Negativity of γ would guarantee instability, but positivity of γ does not guarantee stability as these are necessary conditions. The two conditions $\tau < 0$ and $\Delta < 0$ from above combined with the condition $\Delta - \tau\gamma > 0$, which results from the Routh-Hurwitz criteria (see, *e.g.*, Appendix B of [23]) constitute a set of necessary and sufficient conditions for stability. Unfortunately, the Routh-Hurwitz conditions for (F18) are difficult to analyze due to the large number of parameters and the rational dependence on k.

Elegant conditions sufficient for stability can be obtained by using the Gerschgorin Circle Theorem [24] applied to the columns of $\mathbf{L}$. Application of the theorem guarantees that the eigenvalues of $\mathbf{L}$ lie in the union of three discs in the plane of complex numbers w,

$$\left|w + \left(D_S k^2 + \beta Z^*\right)\right| \leq \left|\frac{2Z^* F \ell^2 k^2}{1 + \ell^2 k^2} + (\beta - \alpha) Z^*\right| + \alpha Z^*, \tag{F20a}$$

$$\left|w + \left(D_Z k^2 + \alpha S^*\right)\right| \leq \frac{2S^* k^2}{1 + k^2} + \alpha S^*, \tag{F20b}$$

$$|w + 1| \leq 1. \tag{F20c}$$

By forcing these discs to lie entirely in the left half-plane, we can guarantee stability. By simple algebra, (F20a) lies in the left half-plane for all k if $\beta > \alpha$ and $D_S > 2Z^* F \ell^2$. The second disc (F20b) lies in the left half plane if $D_Z > 2S^*$. The third disc (F20c) lies in the left half plane no matter what. Hence, the three conditions

$$\beta > \alpha, \quad D_S > 2Z^* F \ell^2, \quad \text{and} \quad D_Z > 2S^*, \tag{F21}$$

are sufficient for stability of the endemic state.

Instability of the endemic equilibrium is possible as well. As mentioned in Section V, the parameters

$$\begin{gathered} \alpha = 1, \quad \beta = 0.1, \quad D_S = 0.1, \quad D_Z = 0.05, \\ c = 0.2, \quad F = 0.3, \quad \ell = 0.3, \quad N = 70, \quad L = 10, \end{gathered} \tag{F22}$$

provide a numerical example of instability. One eigenvalue λ_1 is negative for all k. For the remaining eigenvalues, $\mathrm{Re}(\lambda_{2,3})$ are shown in Figure 7(a) and $\mathrm{Im}(\lambda_{2,3})$ in Figure 7(b). For an intermediate range of k, $\mathrm{Re}(\lambda_{2,3}) > 0$ and $\mathrm{Im}(\lambda_{2,3}) \neq 0$, rendering the endemic equilibrium

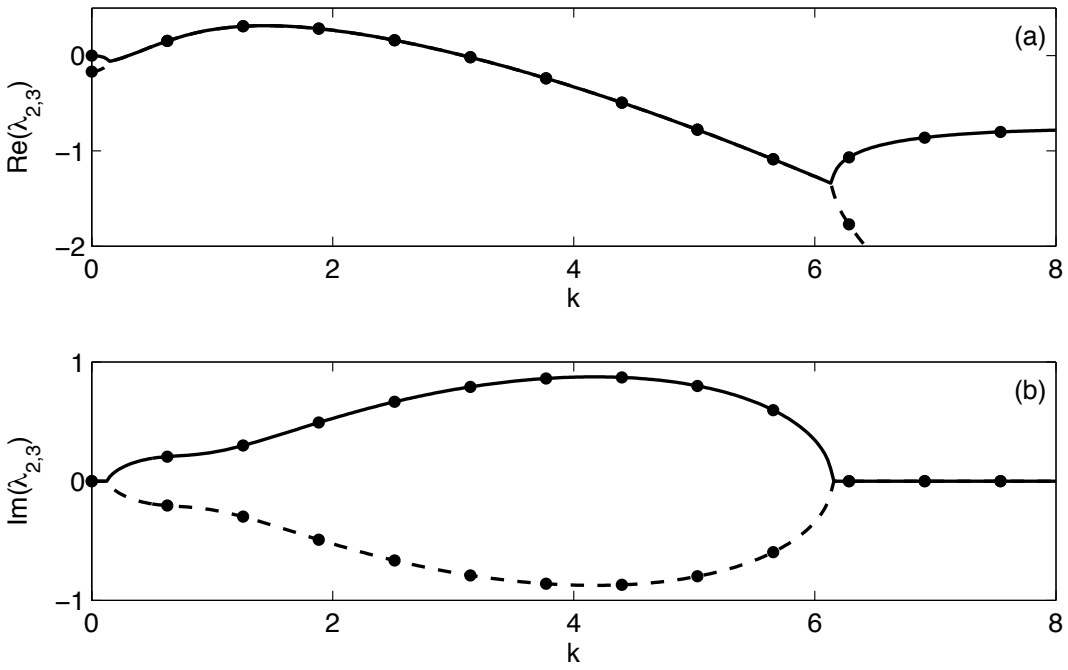

FIG. 7: **Example instability of the endemic state.** (a) Real part of two eigenvalues $\lambda_{2,3}$ for the linearization (F18) of the endemic steady state (23) of the model (18) with parameters (F22). As the spectrum is discrete, data are given by the filled circles; curves are plotted to guide the eyes. The first eigenvalue λ_1 (not shown) is always negative. Since there exist values of the wave number k for which $\mathrm{Re}(\lambda_{2,3}) > 0$, the equilibrium is unstable. (b) Like (a), but depicting $\mathrm{Im}(\lambda_{2,3})$. The eigenvalues are complex for a range of k, including the subset for which $\mathrm{Re}(\lambda_{2,3}) > 0$, indicating an oscillatory instability.

unstable to an oscillatory solution.

---

[1] P. Munz, I. Hudea, J. Imad, and R. J. Smith?, in *Infectious Disease Modelling Research Progress*, edited by J. Tchuenche and C. Chiyaka (Nova Science Publishers, Inc., 2009), chap. 4, pp. 133 – 150.

[2] T. Prentice and L. T. Reinders, Tech. Rep., World Health Organization (2007).

[3] E. F. Keller and L. A. Segel, J. Theor. Biol. **30**, 225 (1971).

[4] A. Okubo, *Diffusion and Ecological Problems* (Springer, New York, 1980).

[5] D. Bernoulli, Mem. Math. Phy. Acad. Roy. Sci. Paris pp. 1–45 (1760).

[6] S. Blower and D. Bernoulli, Rev. Med. Virol. **14**, 275 (2004).

[7] H. W. Hethcote, SIAM Review **42**, 599 (2000).

[8] J. D. Murray, *Mathematical Biology II: Spatial Models and Biomedical Applications*, no. 18 in Interdisciplinary Applied Mathematics (Springer, New York, 2002), 3rd ed.

[9] S. Ruan, in *Mathematics for Life Sciences and Medicine*, edited by Y. Takeuchi, K. Sato, and Y. Iwasa (Springer-Verlag, New York, 2006), vol. 2, pp. 99–122.

[10] J. V. Noble, Nature **250**, 726 (1974).

[11] A. Kallen, P. Arcuri, and J. D. Murray, J. Theor. Bio. **116**, 377 (1985).

[12] J. D. Murray, E. A. Stanley, and D. L. Brown, Proc. Roy. Soc. Lon. B **229**, 111 (1986).

[13] S. Fedotov, Phys. Rev. Lett. **86**, 926 (2001).

[14] J. Medlock and M. Kot, Math. Biosci. **184**, 201 (2003).

[15] D. G. Kendall, in *Mathematics and Computer Science in Biology and Medicine* (H.M. Stationery Off., London, 1965), pp. 213–225.

[16] D. Mollison, Adv. Appl. Prob. **4**, 233 (1972).

[17] D. Mollison, in *Proceedings of the Sixth Berkeley Symposium on Mathematical Statistics and Probability* (Univ. of Calif. Press, Berkeley, CA, 1972), vol. 3, pp. 579–614.

[18] T. Hillen and K. J. Painter, Journal of Mathematical Biology **58**, 183 (2009).

[19] A. Mogilner and L. Edelstein-Keshet, J. Math. Bio. **38**, 534 (1999).

[20] A. J. Leverentz, C. M. Topaz, and A. J. Bernoff, SIAM J. Appl. Dyn. Sys. **8**, 880 (2009).

[21] R. Eftimie, G. de Vries, and M. A. Lewis, Proc. Natl. Acad. Sci. **104**, 6974 (2007).

[22] S. R. Partan and P. Marler, Am. Nat. **166**, 231 (2005).

[23] J. D. Murray, *Mathematical Biology I: An Introduction*, no. 17 in Interdisciplinary Applied Mathematics (Springer, New York, 2002), 3rd ed.

[24] R. A. Brualdi and S. Mellendorf, Amer. Math. Month. **101**, 975 (1994).